

Magnetotransport in Layered Dirac Fermion System Coupled with Magnetic Moments

Yoshiki Iwasaki and Takao Morinari

Graduate School of Human and Environmental Studies, Kyoto University, Kyoto 606-8501, Japan

(Dated: August 17, 2018)

We theoretically investigate the magnetotransport of Dirac fermions coupled with localized moments to understand the physical properties of the Dirac material EuMnBi_2 . Using an interlayer hopping form, which simplifies the complicated interaction between the layers of Dirac fermions and the layers of magnetic moments in EuMnBi_2 , the theory reproduces most of the features observed in this system. The hysteresis observed in EuMnBi_2 can be caused by the valley splitting that is induced by the spin-orbit coupling and the external magnetic field with the molecular field created by localized moments. Our theory suggests that the magnetotransport in EuMnBi_2 is due to the interplay among Dirac fermions, localized moments, and spin-orbit coupling.

Dirac materials have attracted much interest because of their intriguing topological characteristics. Unconventional half-integer quantum Hall effect was observed^{1,2} in graphene³ due to the Landau level structures of Dirac fermions. Unlike conventional metals, the backward scattering is strongly suppressed⁴ due to the Berry phase π , which makes Dirac fermions extremely high mobility carriers.

Recently first-principles calculations predicted that manganese pnictide SrMnBi_2 is a Dirac material, because of the electronic properties of the Bi square net, and subsequently, its dispersion and Fermi surface were observed by angle-resolved photoemission spectroscopy and quantum oscillations.⁵⁻⁷ Interestingly, there are structural and physical similarities between SrMnBi_2 and the 112-type iron-based superconductors.⁶ Antiferromagnetic (AF) ordering of the magnetic moments of Mn occurs below 290 K as suggested by the temperature dependences of magnetization, resistivity, and specific heat.⁶ From the perspective of spintronics application,⁸ it is important to investigate the interplay between Dirac fermions and magnetic moments. In this regard, the Dirac material EuMnBi_2 , which is isostructural with SrMnBi_2 , provides a plausible platform.⁹ Half-integer quantum Hall effect was observed, and the Berry phase π of Dirac fermions was found from the analysis of Shubnikov-de-Haas oscillations.¹⁰

In EuMnBi_2 , the layer of Eu^{2+} with spin $S = 7/2$ is closer to the Bi square net than the layer of Mn-Bi edge sharing tetrahedra. AF ordering of Eu moments around $T_N = 22$ K is suggested from the magnetic susceptibility measurements.⁹ Compared to SrMnBi_2 , the Néel temperature associated with the AF ordering of Mn moments is enhanced to 310 K⁹, which is presumably due to the interaction between Mn moments and Eu moments. Transport measurements demonstrated¹⁰ that the Dirac fermion transport strongly couples to Eu moments. The ordering of Eu moments is AF in the direction of the c axis, which is perpendicular to the layers of Dirac fermions, and ferromagnetic in the ab plane. Below 120 K, both the in-plane resistivity ρ_{xx} and the interlayer resistivity ρ_{zz} show metallic behavior down to T_N with the large anisotropy of $\rho_{zz}/\rho_{xx} \sim 480$ at 50 K.¹⁰ A small drop in ρ_{xx} and an enhancement in ρ_{zz} were observed at $T = T_N$. The effect of coupling between Dirac fermions and Eu moments is seen much clearly under a magnetic field. When the magnetic field is applied in the c axis, ρ_{zz} increases sharply below T_N , and ρ_{zz}/ρ_{xx} exceeds 1 000% at 9 T, while it is about 180% at 0 T. Spin-flop transi-

tion of Eu moments occurs at ~ 5.3 T, and there is a steep increase in ρ_{zz} at the transition point. As the magnetic field was increased, a peak was observed in ρ_{zz} around 20 T.¹⁰ Remarkably, this peak shows a hysteresis between the field-increasing and field-decreasing runs. A hysteretic anomaly was also observed in ρ_{xx} .

In this Letter, we theoretically study the magnetotransport of two-dimensional Dirac fermions coupled with localized moments, and discuss the features experimentally observed in EuMnBi_2 . We calculate the in-plane and interlayer conductivities by using the Kubo formula, assuming a phenomenological form of the interlayer tunneling. In order to explain the hysteresis observed in EuMnBi_2 , the lift of valley degeneracy is taken into account.

Before investigating the magnetotransport of Dirac fermions, we first consider a model for the layers of magnetic moments in EuMnBi_2 . In the absence of a magnetic field, we assume that the localized moments are antiferromagnetically ordered along the c axis in the ground state. Therefore, we denote the even layers of localized moments as A sublayer and the odd layers of localized moments as B sublayer. As shown in Fig. 1, we introduce the angles θ_A and θ_B to describe the direction of the localized moments in A sublayer and B sublayer, respectively. The optimum values of θ_A and θ_B are determined numerically by minimizing the following energy:

$$E = -K(\cos^2 \theta_A + \cos^2 \theta_B) - \mu_B B(\cos \theta_A - \cos \theta_B) - J \cos(\theta_A - \theta_B). \quad (1)$$

Here, K is the anisotropic energy, μ_B is the Bohr magneton, B is the magnetic field, and $J > 0$ is the AF interaction between localized moments. The magnetic field dependences of θ_A and θ_B are shown in Fig. 2. In the spin-flop phase, we found that the energy is given by $E = -J - (\mu_B B)^2 / [2(J - K)]$ and $\cos \theta_A = -\cos \theta_B = \mu_B B / [2(J - K)]$. In terms of the spin flop field B_f and the critical field B_c , above which the spins are fully polarized, K and J are given by $K = \mu_B B_f^2 / (2B_c)$ and $J = \mu_B (B_f^2 + B_c^2) / (2B_c)$, respectively. Substituting the values $B_f \simeq 5$ T and $B_c \simeq 22$ T, which were observed in the experiment,¹⁰ we obtain $K = 0.43$ K and $J = 7.8$ K. In the following, we use this result for the magnetic field dependence of the directions of localized moments.

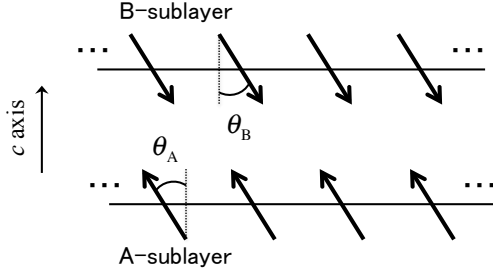


FIG. 1. Layers of localized moments and the definition of the angles, θ_A and θ_B . In each layer, the localized moments are ferromagnetically ordered, while they are antiferromagnetically ordered along the c axis in the ground state. In between the layers of localized moments, there is a single layer of Dirac fermions, which is not shown in the figure.

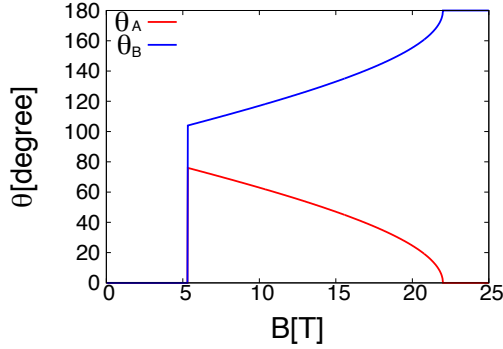


FIG. 2. (Color online) Magnetic field dependence of the angles of localized moments determined by minimizing the energy (1). Because of the anisotropic energy with the parameter K , there is a spin-flop transition at $B \sim 5$ T. For $B > 22$ T, the localized moments are fully polarized.

For the purpose of calculating the in-plane and interlayer conductivities, we need the Landau level wave functions of Dirac fermions. For this, we consider a single valley of Dirac fermions. The presence of another valley and the effect of the lift of its degeneracy are examined later. The Hamiltonian is given by

$$H_D = v \begin{pmatrix} 0 & \pi_x - i\pi_y \\ \pi_x + i\pi_y & 0 \end{pmatrix}, \quad (2)$$

where v is the Fermi velocity of Dirac fermions and $\pi_\alpha = p_\alpha + eA_\alpha$ ($\alpha = x, y$), with p_α and A_α being the momentum operators and the vector potential, respectively. Here, e denotes the electron charge. Based on a first-principles calculation, it was pointed out in Ref. 5 that the Dirac cone in the Bi square net is anisotropic. The largest value of the Fermi velocity is 1.51×10^6 m/s while its smallest value is 1.91×10^5 m/s. Taking the geometrical mean of these values, we assume, $v = 5 \times 10^5$ m/s.

Taking the Landau gauge, $\mathbf{A} = (0, Bx, 0)$, we assume a

plane wave function in the y -direction. The energy of the Landau levels is given by¹¹

$$E_n = \text{sgn}(n)v\sqrt{2e\hbar B|n|}, \quad (3)$$

with integer n . The wave function of the Landau level with n is denoted by $F_n(\mathbf{r})$, where

$$F_0(\mathbf{r}) = \begin{pmatrix} 0 \\ h_0(\mathbf{r}) \end{pmatrix} \quad (4)$$

and

$$F_n(\mathbf{r}) = \frac{1}{\sqrt{2}} \begin{pmatrix} \text{sgn}(n)h_{|n|-1}(\mathbf{r}) \\ h_{|n|}(\mathbf{r}) \end{pmatrix} \quad (5)$$

for $n \neq 0$. The function $h_{|n|}(\mathbf{r})$ is given by

$$h_{|n|}(\mathbf{r}) = i^n \sqrt{\frac{1}{\sqrt{\pi}2^{|n|}|n|!\ell L}} H_{|n|}\left(\frac{x - k\ell^2}{\ell}\right) \times \exp\left[-\frac{1}{2}\left(\frac{x - k\ell^2}{\ell}\right)^2\right] \exp(iky).$$

Here, $H_{|n|}(x)$ is the Hermite polynomial, $\ell = \sqrt{\hbar/e|B|}$ is the magnetic length, and L is the system size in the y direction.

The interlayer conductivity is computed by the Kubo formula.¹² The result is,

$$\sigma_{zz} = \frac{2t_c^2 a_c e^3 \tau}{\pi \hbar^3} B \rho(\mu). \quad (6)$$

Here, t_c is the interlayer hopping, $a_c = 22.5\text{\AA}$ is the lattice constant in the c axis¹⁰, τ is a constant relaxation time, μ is the chemical potential, and $\rho(\epsilon)$ is the spectral function, which has the form of a Lorentz function. From the analysis of the temperature dependence of the Shubnikov-de Haas oscillation amplitude in ρ_{xx} , τ was estimated as $\tau = 3.5 \times 10^{-14}$ s in SrMnBi_2 .⁵ We found that this value is too small for EuMnBi_2 , and therefore we assumed that $\tau = 2.5 \times 10^{-13}$ s to reproduce the Shubnikov-de Haas oscillation observed in Ref. 10.

For the value of μ , we assume $\mu = 1000$ K to reproduce the Shubnikov-de Haas oscillation period that was observed experimentally in ρ_{xx} and ρ_{zz} .¹⁰

In order to apply the formula (6) to EuMnBi_2 , we need to determine the interlayer hopping parameter, t_c . In between the Dirac fermion layers of EuMnBi_2 , there are three layers: two layers of Eu moments and one layer composed of Mn^{2+} ions and Bi^{3-} ions. The parameter t_c depends on not only the directions of Eu moments and Mn moments but also the interaction between Dirac fermions and Bi^{3-} ions. We note that those Bi^{3-} ions are different from Bi^{1-} ions forming the layers of Dirac fermions.^{9,10} In order to avoid this complication, here we assume that the magnetic layers between Dirac fermion layers consist of a single component of localized moments, whose AF order is described by θ_A and θ_B , above. Then, in the spin-flop phase, t_c depends on $\theta_B = \pi - \theta_A$. Apparently, the interlayer hopping t_c is maximum when the localized moments are fully polarized, while it is minimum in the AF phase. As

a simple phenomenological model, we assume the following form

$$t_c \propto 1 - \cos \frac{\theta_B}{2}. \quad (7)$$

The proportionality constant is chosen such that t_c takes the value of 200 K in the fully polarized state of localized moments.

The Kubo formulae for the in-plane conductivity and Hall conductivity are given by

$$\sigma_{xx} = \frac{e^2 \hbar}{2\ell^2 a} \sum_{n,n'} \rho(\mu - E_n) \rho(\mu - E_{n'}) |\langle \mathbf{F}_n | \sigma_x | \mathbf{F}_{n'} \rangle|^2, \quad (8)$$

$$\sigma_{xy} = \frac{\hbar e^2 v^2}{\pi a \ell^2} \sum_{n,n'} \frac{f(\mu - E_n)}{(E_n - E_{n'})^2} \text{Im} \langle \mathbf{F}_n | \sigma_x | \mathbf{F}_{n'} \rangle \langle \mathbf{F}_{n'} | \sigma_y | \mathbf{F}_n \rangle, \quad (9)$$

respectively. Here, $a = 4.5 \text{ \AA}$ is the lattice constant in the plane,⁹ and σ_x and σ_y are Pauli matrices. The function $f(x)$ is defined by $f(x) = 1/2 + \arctan(x/\Gamma)/\pi$, where $\Gamma = \hbar/\tau$ is a constant parameter describing the broadening of Landau levels due to impurity scatterings. The resistivity is computed numerically using the formula given by $\rho_{xx} = \sigma_{xx}/(\sigma_{xx}^2 + \sigma_{xy}^2)$, $\rho_{yx} = \sigma_{xy}/(\sigma_{xx}^2 + \sigma_{xy}^2)$, and $\rho_{zz} = 1/(\sigma_{zz} + \sigma_0)$. Here, parameter $\sigma_0 = 0.01$, which is associated with impurity scattering, is introduced to reproduce the experimentally observed ρ_{zz} .¹⁰

The result obtained by including the Zeeman energy splitting is shown in Fig. 3. Here, the magnetic field is normalized by introducing parameter $B_F \equiv \mu^2/(2e\hbar v^2) \simeq 23 \text{ T}$, which is the frequency of Shubnikov-de-Haas oscillations. The inverse of the Hall resistivity ρ_{yx} shows a half-integer quantum Hall effect, as shown in Fig. 3(a). Some deviations from the ideal quantum Hall plateaus occur due to the broadening factor, Γ , and similar features were seen in the experiment.¹⁰ ρ_{xx} and ρ_{zz} are shown in Fig. 3(b) and (c), respectively. The positions of the peaks of ρ_{xx} and the minimum of ρ_{zz} reflect the Landau level structure.¹⁰ The density of states takes a large value when the chemical potential is equal to a Landau level energy upon varying the magnetic field. Reflecting this, ρ_{zz} shows a dip while ρ_{xx} shows a peak around integer values of B/B_F . The splitting of peaks in ρ_{xx} and that of dips in ρ_{zz} are due to the lift of the level degeneracy. Here, the degeneracy is associated with the spin degrees of freedom. The result shown in Fig. 3 qualitatively agrees with the experiment.¹⁰ In the experiment, the splitting of the peak in ρ_{xx} is observed at $B_F/B = 1$. Furthermore, the peak at $B_F/B < 1$ is larger than that at $B_F/B > 1$. This is consistent with the experiment as well. In the experiment, the splitting of the peak in ρ_{xx} is not observed at $B_F/B = 2$. However, the second derivative of ρ_{xx} with the minus sign, obtained from the experimental data, shows the splitting of the peak. The positions of the minimum in ρ_{zz} , shown in Fig. 3(c), is also consistent with the experiment.¹⁰ However, there is an important difference: the theory suggests the presence of two dips and one small peak around $B_F/B = 1$, whereas this peak is much larger in the experiment. It is unlikely that the peak appears as a result of splitting of the dip.

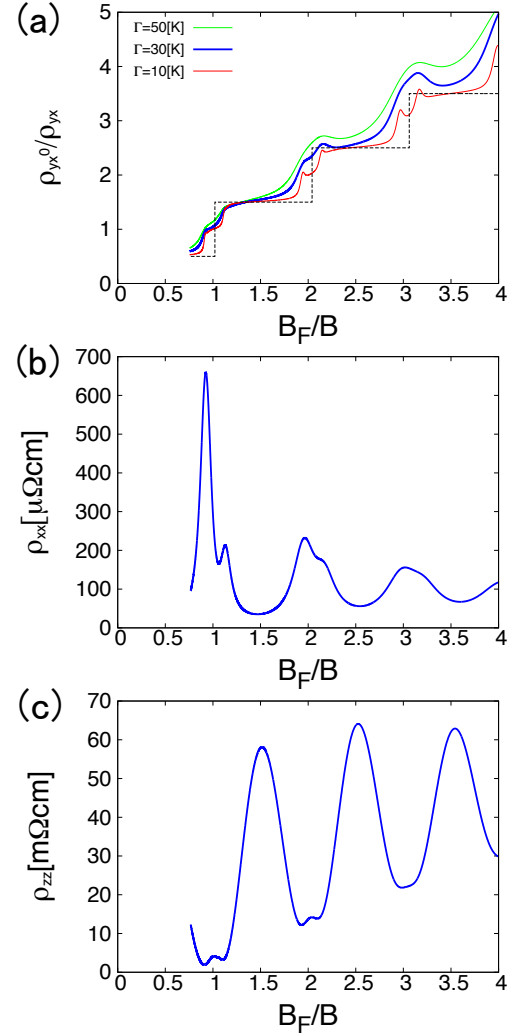


FIG. 3. (Color online) Normalized inverse Hall resistivity ρ_{yx}^0/ρ_{yx} (a), in-plane resistivity ρ_{xx} (b), and interlayer resistivity ρ_{zz} (c) versus the inverse of the normalized magnetic field. Here, we take $\rho_{yx}^0 = 1.1 \times 10^{-3} \Omega\text{-cm}$. B_F is the frequency of Shubnikov-de-Haas oscillations defined in the main text. Here, we plot the values in $B < B_c$ where t_c , which is given by Eq. (7), is finite. In the panel (a) we plot ρ_{yx} for different values of Γ and the idealized case is shown in the dashed line.

Now we consider the effect of valley splitting. The Hamiltonian is given by

$$H = v \begin{pmatrix} \tilde{\Delta} & \pi_x - i\pi_y & 0 & 0 \\ \pi_x + i\pi_y & \tilde{\Delta} & 0 & 0 \\ 0 & 0 & -\tilde{\Delta} & \pi_x + i\pi_y \\ 0 & 0 & \pi_x - i\pi_y & -\tilde{\Delta} \end{pmatrix}. \quad (10)$$

Here, $\tilde{\Delta} = \Delta/v$. The parameter Δ is the energy gap created by the valley splitting. The Landau level wave functions for another valley is obtained by simply multiplying τ_x , which is the Pauli matrix in the sublattice space in the layer of Dirac fermions, to the two-component spinors, Eqs. (4) and (5),

from the left hand side. Experimentally, it is suggested that Δ depends linearly on the magnetic field.¹³ We assume that the valley splitting occurs through the interaction with the localized moments, and the origin of the hysteresis is in the system of localized moments. Therefore, we use different proportionality constants for the field-decreasing run and the field-increasing run. We use $1.6\mu_B$ for the former and $1.5\mu_B$ for the latter. We used these values to reproduce the two-peak structure of ρ_{xx} that was observed around $B_F/B = 1$ in the experiment.¹⁰ The difference of $0.1\mu_B$ in these values is taken such that the numerical calculation reproduces the experimentally observed difference in peak values, which are associated with the hysteresis, of ρ_{xx} at $B_F/B \sim 1.2$. The numerical calculation result is shown in Fig. 4. The difference between the two cases is seen in ρ_{xx} around $B_F/B \sim 1$, which is similar to that observed in the experiment.¹⁰ However, the theory failed to reproduce the experimentally observed feature in ρ_{zz} around $B_F/B \sim 1$.¹⁰ This discrepancy is probably due to the form of the interlayer hopping Eq. (7). We need a more realistic t_c than Eq. (7) to explain the experiment, which is left for future research.

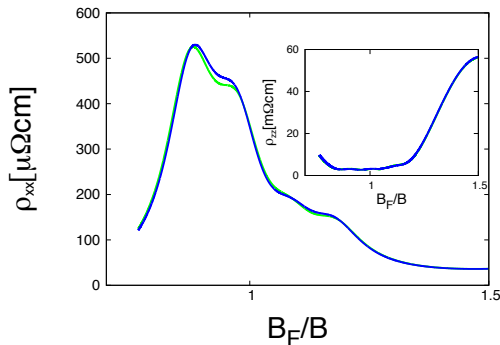


FIG. 4. (Color online) In-plane resistivity ρ_{xx} and interlayer resistivity ρ_{zz} (inset) versus the inverse of the normalized magnetic field. The green lines indicate the result with $\Delta = 1.6\mu_B$, and the blue lines indicate the result with $\Delta = 1.5\mu_B$.

An important question, which needs to be considered, is the mechanism of valley splitting. If we recall that bismuth plays a major role in topological insulators^{14,15} and the key is strong spin-orbit coupling, one possible scenario is that valley

splitting occurs through spin-orbit coupling, $i\lambda \cdot \sigma$ with $\lambda = (\lambda_x, \lambda_y, \lambda_z)$. Generally, λ depends on the wave vector of Dirac fermions; however, if we focus on a single Dirac point, then the Hamiltonian is given by

$$H_\lambda = \begin{pmatrix} -\mu_B B_{\text{eff}} & 0 & i\lambda_z & i\lambda_x + \lambda_y \\ 0 & \mu_B B_{\text{eff}} & i\lambda_x - \lambda_y & -i\lambda_z \\ -i\lambda_z & -i\lambda_x - \lambda_y & -\mu_B B_{\text{eff}} & 0 \\ -i\lambda_x + \lambda_y & i\lambda_z & 0 & \mu_B B_{\text{eff}} \end{pmatrix}. \quad (11)$$

Here, we have included in B , the effect of the molecular fields created by localized spins, and we denote the effective magnetic field by B_{eff} . The eigenvalues of this Hamiltonian is obtained exactly as, $E^{(\pm, \pm)} = \pm \sqrt{(\lambda_z \pm \mu_B B_{\text{eff}})^2 + \lambda_x^2 + \lambda_y^2}$. For $|\lambda_z| \gg |\mu_B B_{\text{eff}}|$, we obtain, $E^{(\pm, \pm)} \simeq \pm \lambda \pm \frac{\lambda_z}{\lambda} \mu_B B_{\text{eff}}$. Therefore, in this scenario, the parameter Δ is given by

$$\Delta = \frac{2\lambda_z}{\lambda} \mu_B B_{\text{eff}}. \quad (12)$$

If $2\lambda_z/\lambda \sim 1$, then the above calculation is justified. Furthermore, the slight change in Δ in the field-decreasing run and the field-increasing run is associated with the hysteresis in the system of localized moments.

To conclude, we have investigated the magnetotransport of two-dimensional Dirac fermions coupled with localized moments, and compared the theoretical result with the experimental result for EuMnBi_2 . Most of the features observed in EuMnBi_2 is understood by our model with interlayer hopping Eq. (7). The hysteresis observed in ρ_{xx} and ρ_{zz} can be associated with the valley splitting resulting from the spin-orbit coupling and the coupling between Dirac fermions and localized moments. However, the theory failed to explain the feature around the Landau level with the index $n = 1$. Presumably, this discrepancy arises from the complicated interaction between Dirac fermions and the magnetic layer in EuMnBi_2 .

ACKNOWLEDGMENTS

We thank H. Masuda and S. Sato for helpful discussions. This work was supported by a Grant-in-Aid for Scientific Research (B) (No. 25287089), from the Ministry of Education, Culture, Sports, Science, and Technology, Japan.

¹ K. S. Novoselov, A. K. Geim, S. V. Morozov, D. Jiang, M. I. Katsnelson, I. V. Grigorieva, S. V. Dubonos, and A. A. Firsov, *Nature* **438**, 197 (2005).
² Y. Zhang and Y.-W. Tan, H. L. Stormer and P. Kim, *Nature* **438**, 201 (2005).
³ A. K. Geim and K. S. Novoselov, *Nat. Mater.* **6**, 183 (2007).
⁴ T. Ando, T. Nakanishi, and R. Saito, *J. Phys. Soc. Jpn.* **67**, 2857 (1998).
⁵ J. Park, G. Lee, F. Wolff-Fabris, Y. Y. Koh, M. J. Eom, Y. K. Kim, M. A. Farhan, Y. J. Jo, C. Kim, J. H. Shim and J. S. Kim, *Phys.*

Rev. Lett. **107**, 126402 (2011).

⁶ J. K. Wang, L. L. Zhao, Q. Yin, G. Kotliar, M. S. Kim, M. C. Aronson, and E. Morosan, *Phys. Rev. B* **84**, 64428 (2011).
⁷ G. Lee, M. A. Farhan, J. S. Kim, and J. H. Shim, *Phys. Rev. B* **87**, 245104 (2013).
⁸ Žutić, J. Fabian, and S. Das Sarma, *Rev. Mod. Phys.* **76**, 323 (2004).
⁹ A. F. May, M. A. McGuire, B. C. Sales, *Phys. Rev. B* **90**, 075109 (2014).

- ¹⁰ H. Masuda, H. Sakai, M. Tokunaga, Y. Yamasaki, A. Miyake, J. Shioyai, S. Nakamura, S. Awaji, A. Tsukazaki, H. Nakao, Y. Murakami, T. H. Arima, Y. Tokura, and S. Ishiwata, *Sci. Adv.* **2**, e1501117 (2016).
- ¹¹ A. H. Castro Neto, F. Guinea, N. M. R. Peres, K. S. Novoselov, and A. K. Geim, *Rev. Mod. Phys.* **81**, 109 (2009).
- ¹² T. Osada, *J. Phys. Soc. Jpn* **77**, 084711 (2008).
- ¹³ H. Masuda, private communication.
- ¹⁴ M. Z. Hasan and C. L. Kane, *Rev. Mod. Phys.* **82**, 3045 (2010).
- ¹⁵ X.-L. Qi and S.-C. Zhang, *Rev. Mod. Phys.* **83**, 1057 (2011).